

# Matrix-IR Spectroscopic Investigations of the Thermolysis and Photolysis of Diazoamides

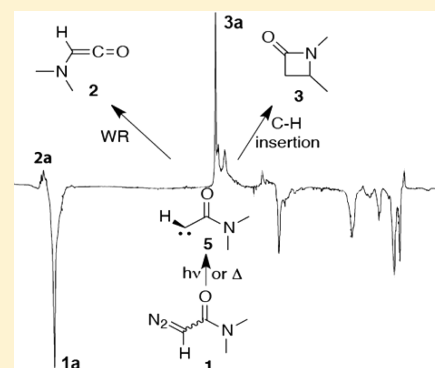
Curt Wentrup,<sup>\*,†</sup> Hervé Bibas,<sup>†</sup> Arvid Kuhn,<sup>†</sup> Ullrich Mitschke,<sup>†</sup> and Mark C. McMills<sup>‡</sup>

<sup>†</sup>School of Chemistry and Molecular Biosciences, The University of Queensland, Brisbane, Queensland 4072, Australia

<sup>‡</sup>Department of Chemistry and Biochemistry, Ohio University, 380 Clippinger Laboratories, Athens, Ohio 45701, United States

**S** Supporting Information

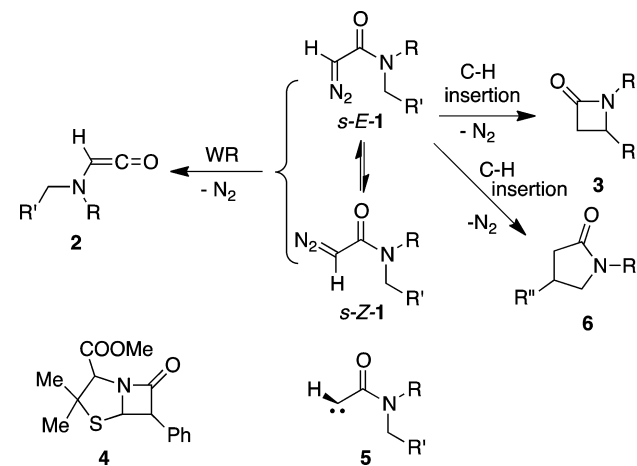
**ABSTRACT:** Matrix photolysis of *N,N*-dialkyldiazoacetamides **1a–d** at 7–10 K results in either the formation of C–H insertion products (in case of *N,N*-dimethyl and *N,N*-diethyl diazoamides) or almost exclusive Wolff rearrangement to ketenes (in the case of the cyclic diazoamides *N*-(diazoacetyl)azetidone and *N*-(diazoacetyl)pyrrolidone). This can be ascribed to higher activation barriers for the approach of the singlet carbene p orbital in **5** (or of the diazo carbon in an excited state of **1**) to the stronger and “tied back” nature of the C–H bonds in the cyclic substituents. In contrast, flash vacuum thermolysis (FVT) of diazoamides **1a–d**, in which reactions of excited states are excluded, gives rise to clean C–H insertion with only minor Wolff rearrangement to ketenes.



## INTRODUCTION

Diazoacetamides **1** may be expected to undergo photochemically or thermally induced Wolff rearrangement<sup>1</sup> (WR) to form ketenes **2** (Scheme 1).<sup>2</sup> However, insertion into substituents at

### Scheme 1. Wolff Rearrangement (WR) and C–H Insertion Reactions of Diazoamides



the amide nitrogen may compete with the Wolff rearrangement,<sup>3,4</sup> leading to the formation of  $\beta$ - and  $\gamma$ -lactams **3** and **6** (Scheme 1). Both reactions may proceed either via the *s*-Z or *s*-E conformers of **1** or via the carbenes **5**. The formation of  $\beta$ -lactams is synthetically interesting and has been used in the preparation of methyl penicillanate (**4**)<sup>5</sup> and many related compounds, especially by employing rhodium- or ruthenium-

catalyzed reactions; varying ratios of  $\beta$ - or  $\gamma$ -lactams have been obtained from substituted diazoamides under these conditions.<sup>6</sup> The C–H insertion reaction usually dominates for diazoamides, reducing the Wolff rearrangement to trace amounts, if it is present at all.<sup>3,4,7</sup> In this regard diazoamides differ from the related diazo esters, which readily form ketenes both photochemically and thermally. In spite of a statement to the contrary,<sup>1b</sup> alkoxy groups do migrate in thermal Wolff rearrangements under FVT conditions,<sup>8,9</sup> and we will show that amino groups migrate as well.

Rando<sup>3</sup> explained the preference for diazoamides to undergo intramolecular C–H insertion on photolysis with the conformational differences between the ester and the amide bonds: the planar peptide-type bond in the diazoamides should bring one N substituent into sufficient proximity to the carbene center and hence facilitate intramolecular insertion.

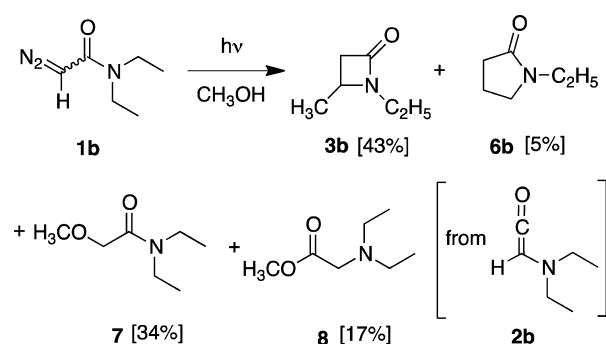
The photochemical decomposition of *N,N*-diethylacetamide (**1b**) with near-UV light in various solvents afforded almost quantitative transformation to the two C–H insertion products 1-ethyl-4-methyl-2-azetidone (**3b**) and 1-ethyl-2-pyrrolidinone (**6b**).<sup>3b</sup> In protic solvents such as methanol, the formation of  $\gamma$ -lactam **6b** decreased sharply, mainly in favor of the O–H insertion product **7** (Scheme 2). In addition, ester **8** was also found, thereby indicating a non-negligible contribution of WR to ketene **2b** under these conditions (Scheme 2).

Tomioka et al. refined these observations mechanistically and posited the participation of a noncarbenic process in the intramolecular C–H insertion.<sup>4</sup> Investigating the relative ratio of all products under various conditions, in particular by

Received: August 2, 2013

Published: October 8, 2013

### Scheme 2. Products of Solution-Phase Photolysis of Diazoamide 1b



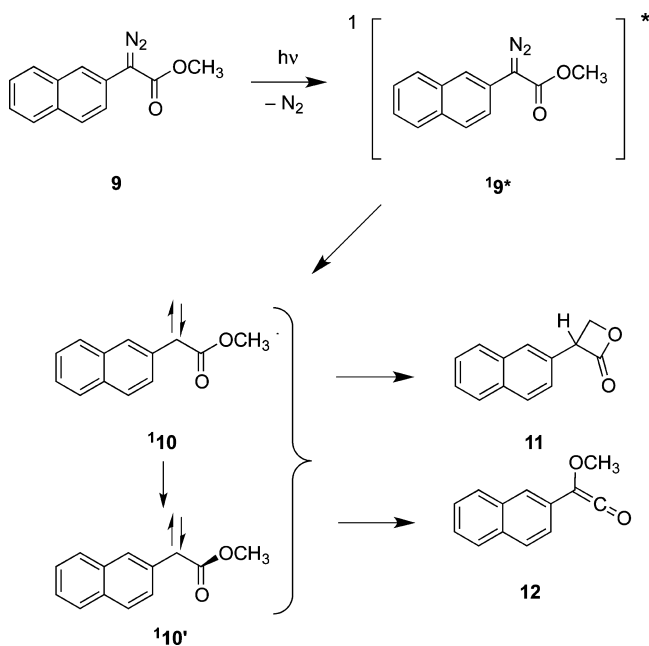
examining the effects of sensitizers and quenchers on the product distributions, the authors concluded that the  $\beta$ -lactam **3b** and the Wolff rearrangement product **8** are formed directly from the singlet excited state of *N,N*-diethyldiazoacetamide ( $^1\mathbf{1b}^*$ ), whereas the formation of  $\gamma$ -lactam **6b** and the O–H insertion product **7** should involve a free singlet carbene.<sup>4a</sup>

Recent femtosecond time-resolved laser flash photolysis studies demonstrated that both the  $\beta$ - and the  $\gamma$ -lactams **3b** and **6b** are in fact formed from  $^1\mathbf{1b}^*$ , i.e. by reaction in the excited state (RIES process), but the  $\gamma$ -lactam is also formed from the singlet carbene  $^1\mathbf{5}$ . The product of methanol addition, **7**, is also formed from  $^1\mathbf{5}$ , but there was no information on the ketene **2b** or its methanol trapping product **8**.<sup>10</sup>

In contrast, femtosecond time-resolved infrared studies on the naphthyl-substituted diazo ester **9** clearly revealed that both the ketene **12** and the  $\beta$ -lactone **11** are formed entirely from carbene **10** with very little if any contribution from the excited singlet state  $^1\mathbf{9}^*$  (Scheme 3).<sup>11</sup> The singlet carbene  $^1\mathbf{10}$  is born in the planar structure—like the diazo compound **9**—but relaxes to the nonplanar form  $^1\mathbf{10}'$  on a femtosecond time scale.<sup>10</sup>

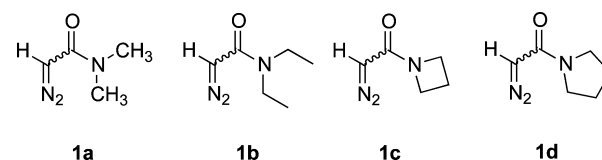
Almost nothing is known about the thermal decomposition of diazoamides, where RIES reactions can obviously be

### Scheme 3. Photolysis of Diazo Ester 9



excluded. In order to cast more light on these reactions, we have investigated the thermolyses and photolyses of diazoamides **1a–d** (Scheme 4) by matrix-isolation IR spectroscopy.

### Scheme 4. Diazoamides Investigated in This Paper<sup>a</sup>



<sup>a</sup>No stereochemical preferences are implied (*s-E* and/or *s-Z*); see text.

## RESULTS

**Photochemical Decomposition of Matrix-Isolated Diazoamides 1a–d.** Diazoamides can exist in *s-E* and *s-Z* conformations (Scheme 1), but in contrast to the diazo esters, the *s-Z* conformers are energetically preferred, although the calculated energy difference is small (2.75 kcal/mol for *N,N*-dimethyldiazoacetamide (**1a**) at the B3LYP/6-31G\*\* level (see the Supporting Information)). This can be ascribed to a steric interaction between the  $\text{N}_2$  moiety and an alkyl group in the *s-E* form. The diazo bands in the matrix IR spectra of the diazoamides **1a–d** are uniformly sharp, thereby indicating that one major conformer is present (see Figure 1 and

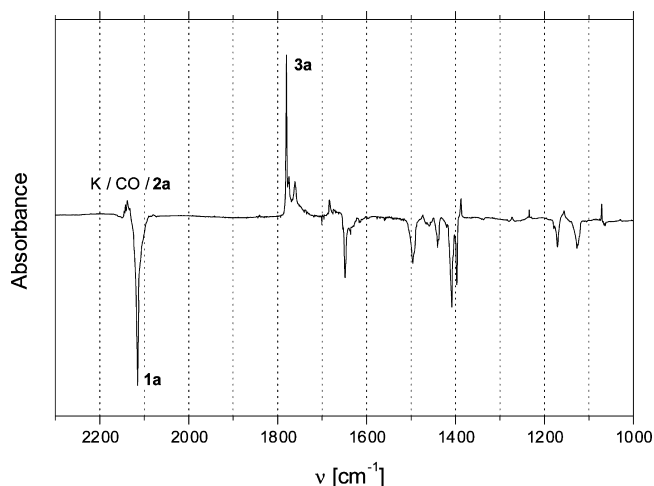
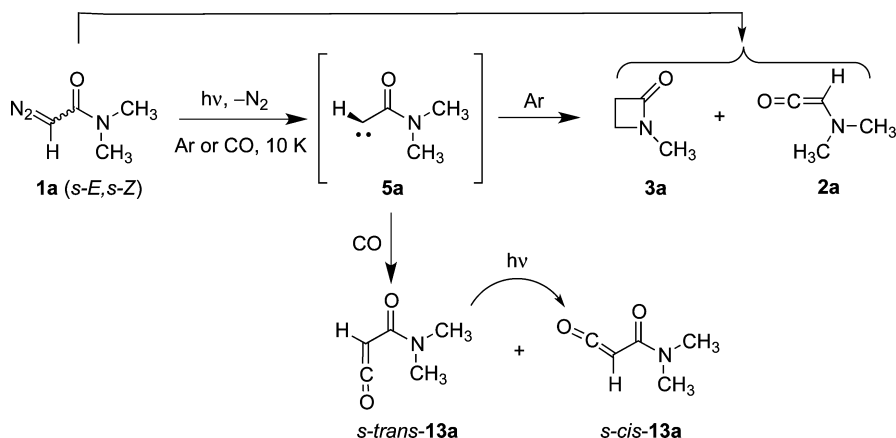


**Figure 1.** IR difference spectrum after irradiation of *N,N*-dimethyldiazoacetamide (**1a**) (2115, 1649, 1496, 1409, 1397  $\text{cm}^{-1}$ ) at  $\lambda \geq 305$  nm for 3.5 h in Ar matrix at 7 K: (bottom) disappearing bands of **1a**; (top) appearing bands of *N*-methylazetidinone (**3a**) (1780  $\text{cm}^{-1}$ ) and *N,N*-dimethylaminoketene (**2a**) (2132  $\text{cm}^{-1}$ ; calculated value 2137  $\text{cm}^{-1}$  (Table 1)). Peaks due to ketene  $\text{CH}_2\text{CO}$  (K) at 2142  $\text{cm}^{-1}$  and CO at 2138  $\text{cm}^{-1}$  arise from the photochemical decomposition of **3a**.

subsequent figures). The IR spectra of the matrix-isolated **1a–d** agree best with the calculated IR spectra of the *s-Z* conformers (see the Supporting Information), which are therefore the likely source of the observed chemistry. In the FVT reactions described in Thermal Decomposition of Diazoamides **1a–d**, however, the small energy barrier between the two conformers is easily overcome, so that either conformer may be involved.

***N,N*-Dimethyldiazoacetamide (1a).** Photolysis of matrix-isolated **1a** at  $\lambda \geq 305$  nm results in the formation of *N*-methylazetidinone (**3a**) (strong absorption at 1780  $\text{cm}^{-1}$ )

Scheme 5. Matrix Photolysis of Dizoamide 1a and Trapping of Carbene 5a with CO



together with a small amount of dimethylaminoketene (2a) ( $2132\text{ cm}^{-1}$ ; Scheme 5 and Figure 1). The identity of the  $\beta$ -lactam 3a was ascertained by deposition of an authentic sample. The IR spectra of all the aminoketenes 2a–d examined here are dominated by the strong  $\text{C}=\text{C}=\text{O}$  stretch around  $2130\text{ cm}^{-1}$  (absolute intensities 500–600  $\text{km/mol}$ ), so that all other absorptions at lower frequencies have relative intensities below 6% of the ketene band (see Table 1 and the Supporting Information).

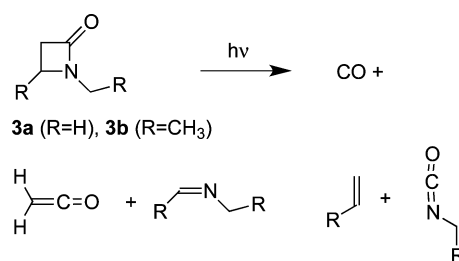
Table 1. Comparison of Calculated (B3LYP/6-31G(d)) and Observed (Ar Matrix, 10 K) Characteristic IR Bands of Ketenes 2, Azetidiones 3, and Pyrrolidinones 6

	$\nu_{\text{calcd}}/\text{cm}^{-1}$ ( $I/\text{km mol}^{-1}$ ) <sup>a</sup>	$\nu_{\text{exptl}}/\text{cm}^{-1}$
Ketenes		
2a <sup>b</sup>	2137 (579)	2132
2b <sup>c</sup>	2104/2101 (499/490)	2132
2c <sup>d</sup>	2133 (660)	2133
2d <sup>e</sup>	2135 (632)	2134
Azetidiones		
3a	1806 (503)	1782
3b	1799 (512)	1775
3c	1813 (401)	
3d	1806 (458)	1785
Pyrrolidinones		
6b	1737 (348)	1715
6d	1804 (289)	

<sup>a</sup>Wavenumbers scaled by 0.9613. <sup>b</sup>No band at lower frequency with intensity  $I > 6\%$  of the ketene band. <sup>c</sup>Two different conformers; no bands at lower frequency with  $I > 6\%$ . <sup>d</sup>No bands at lower frequency with  $I > 2\%$ . <sup>e</sup>No bands at lower frequency with  $I > 3\%$  of ketene band.

Prolonged irradiation at  $\lambda \geq 305\text{ nm}$  or short irradiation at shorter wavelength (254 nm) gives rise to increased intensities of signals at 2142 and  $2138\text{ cm}^{-1}$ , which are assigned to ketene ( $\text{CH}_2\text{CO}$ ) and carbon monoxide, respectively (Figure 1). Other bands characteristic of ketene were present at 2086, 1380, 114, and  $973\text{ cm}^{-1}$ , and the compound was characterized securely by direct comparison with an authentic sample. Ketene is most probably formed in a photochemically induced [2 + 2] cycloreversion of  $\beta$ -lactam 3a (Scheme 6). (Further information on the cycloreversions is given in Thermal Decomposition of Diazoamides 1a–d.) The presence of carbene 5a was confirmed by trapping with CO. This procedure has been used previously to demonstrate the formation of alkoxy carbonylcar-

Scheme 6. Products of Photodecomposition of  $\beta$ -Lactams 3a,b



benes and arylcarbenes from diazo compounds.<sup>9,11a,12</sup> Stabilized diaminocarbenes do not react with CO, but the more reactive acylaminocarbenes do.<sup>13</sup> Here, the photolysis of 1a in a carbon monoxide matrix yielded both *s-cis* and *s-trans*  $\alpha$ -oxoketene conformers 13a together with an approximately equal amount of 3a (Figure 2). This result is compatible with (but does not demand) the coexistence of carbenic and noncarbenic photochemical processes, the latter leading to C–H insertion. Prolonged irradiation caused complete conversion of *s-trans*-13a to the *s-cis*-13a conformer, in which there is less steric interaction between ketene and dimethylamino groups (Figure 2).

*N,N*-Diethyldiazoacetamide (1b). The preference for C–H insertion is also observed for the *N,N*-diethyl analogue 1b. The photolysis of matrix-isolated 1b yielded  $\beta$ -lactam 3b as the predominant product together with smaller amounts of  $\gamma$ -lactam 6b and ketene 2b ( $2132\text{ cm}^{-1}$ ) (Scheme 7 and Figure 3). Larger-scale Figures S1–S3 in the Supporting Information clearly show the bands of 3b, 6b, and 2b developing during the first 15 min of photolysis ( $\lambda \geq 290\text{ nm}$ ). Already after 15 min of photolysis a peak due to CO ( $2137\text{ cm}^{-1}$ ) appears next to the ketene peak ( $2132\text{ cm}^{-1}$ ) due to photochemical decomposition.

Further irradiation at  $\lambda \geq 290\text{ nm}$  or—faster—at  $\lambda \geq 190/254\text{ nm}$  (low-pressure Hg lamp without filter) causes decomposition of the  $\beta$ -lactam 3b to two sets of [2 + 2] cycloreversion products together with increased formation of CO (Scheme 6 and Figure 4).<sup>14</sup>

Thus, new bands at  $2142\text{ cm}^{-1}$  and a series of bands at 2289, 2279, and  $2266\text{ cm}^{-1}$  are assigned to ketene ( $\text{CH}_2\text{CO}$ ) and ethyl isocyanate, respectively.<sup>14</sup> The ketene band is seen as a weak shoulder on the high-frequency side of CO ( $2138\text{ cm}^{-1}$ ).

*N*-(Diazoacetyl)azetidine (1c). In sharp contrast to the clear prevalence of C–H insertion in the photolyses of open-chain

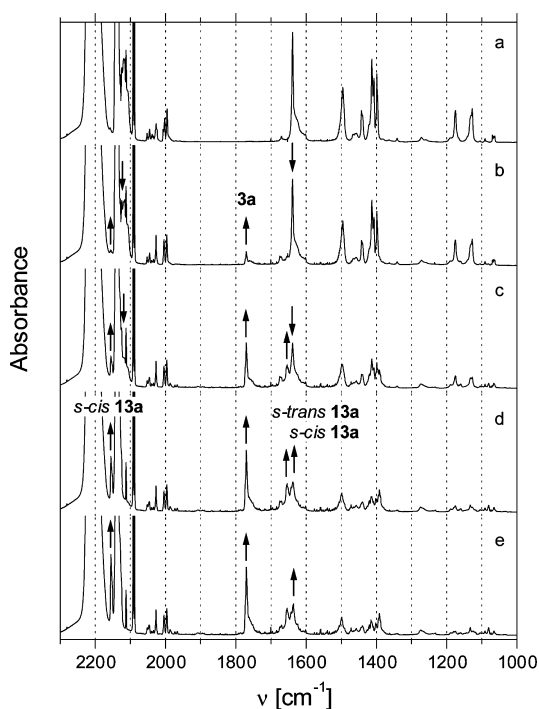
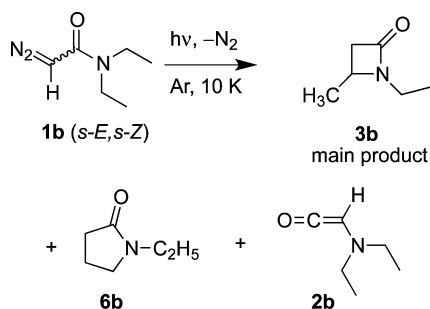


**Figure 2.** Course of the photochemical decomposition of *N,N*-dimethyldiazoacetamide (**1a**) (2119, 1638  $\text{cm}^{-1}$ ) in a CO matrix at 8 K at  $\lambda \geq 305$  nm: (a) deposition spectrum; (b) spectrum after 1 h irradiation at  $\lambda \geq 305$ –310 nm; (c–e) spectra after an additional 10 min (c), 21 min (d), and 35 min (e) of irradiation at  $\lambda$  254 nm. The assignment of the bands is supported by B3LYP/6-31G(d) calculations. The disappearance of **1a** (2119, 1638  $\text{cm}^{-1}$ ) and appearance of **3a** (1770  $\text{cm}^{-1}$ ), *s-trans*-**13a** (2131, 1683  $\text{cm}^{-1}$ ) (appearing first), and *s-cis*-**13a** (2155, 1654  $\text{cm}^{-1}$ ) (appearing later) are indicated by arrows. The absorption of the ketene function of *s-trans*-**13a** (calculated at 2130  $\text{cm}^{-1}$ ) is hidden under the neighboring CO band (see the Supporting Information for calculated data).

#### Scheme 7. Matrix Photolysis of Diethyldiazoacetamide (**1b**)



*N,N*-dialkyl diazoamides **1a,b**, the incorporation of the amide nitrogen into a small heterocycle such as *N*-(diazoacetyl)-azetidine (**1c**) causes predominant conversion to the WR product, the aminoketene **2c** (Scheme 8 and Figure 5).

The possible C–H insertion products, viz. the strained bicyclic  $\beta$ -lactam **3c** and 1-azatricyclo[2.1.1]hexan-2-one (**6c**), were not detected. The existence of carbene **5c** as an intermediate was again proved in a trapping experiment with CO (Scheme 8 and Figure 6). At first, the resulting azetidylcarbonylketene **13c** is formed in the *s-trans* conformation, which is gradually transformed to the *s-cis* conformer upon prolonged irradiation. Notably, the aminoketene **2c** was not observable in this experiment. Because the

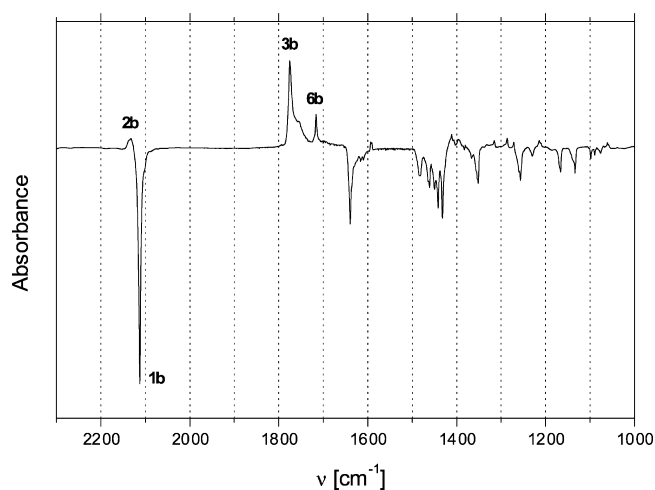


**Figure 3.** IR difference spectrum after irradiation of *N,N*-diethyldiazoacetamide (**1b**) (2112, 1639  $\text{cm}^{-1}$ ) at  $\lambda \geq 290$  nm for 15 min in an Ar matrix at 8 K: (bottom) disappearing bands of **1b**; (top) appearing bands of 1-ethyl-4-methyl-2-azetidinone (**3b**) (1775, 1755  $\text{cm}^{-1}$ ), 1-ethyl-2-pyrrolidinone (**6b**) (1716  $\text{cm}^{-1}$ ), and *N,N*-diethylaminoketene (**2b**) (2132  $\text{cm}^{-1}$ ).

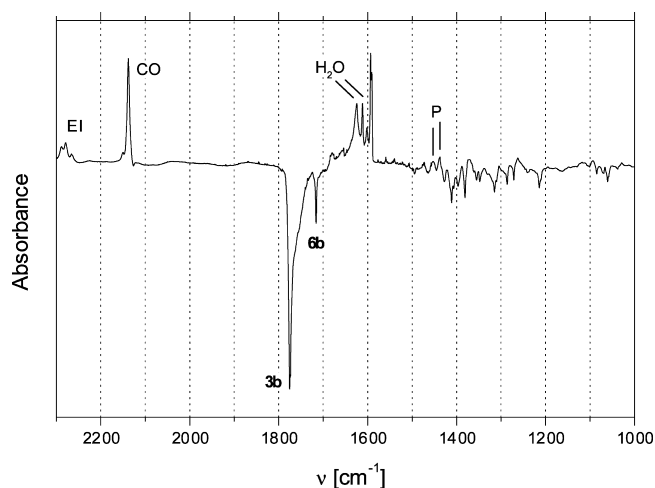


**Figure 4.** IR difference spectrum after irradiating the mixture of  $\beta$ -lactam **3b**,  $\gamma$ -lactam **6b**, and ketene **2b** (Figure 3) for another 3 h at  $\lambda$  190/254 nm in an argon matrix at 8 K: (top) appearing bands of carbon monoxide (CO), ethyl isocyanate (EI), and propene (P);<sup>14</sup> (bottom) disappearing bands of **3b**, **6b**, and **2b** (2132  $\text{cm}^{-1}$ ).

signal could be hidden under the CO band, the experiment was repeated with a matrix composed of 10% CO in Ar. The same results were obtained, and ketene **2c** was not observable. This makes it possible that carbene **5c** is involved in the photochemical WR to **2c**.

*N*-(Diazoacetyl)pyrrolidine (**1d**). The high strain energies of the bicyclo[2.2.0] and [2.1.1] derivatives **3c** and **6c** and/or the more difficult approach of the diazo carbon or carbene to the tied-back methylene groups apparently disfavor the intramolecular C–H insertion (see further in the Discussion). Therefore, it was of interest to examine the pyrrolidine analogue **1d**. Here, a weak absorption at 1785–1761  $\text{cm}^{-1}$  (Figure 7) suggests the formation of a minor amount of  $\beta$ -lactam **3d**, which has been identified securely in the FVT reaction of **1d**, where it is formed in much larger amount (see Figure 11 below). Compound **6d** is unknown, but the calculated carbonyl absorptions of **3d** and **6d** are identical

## Scheme 8. Matrix Photolysis of Diazoamide 1c and Trapping of Carbene 5c with CO

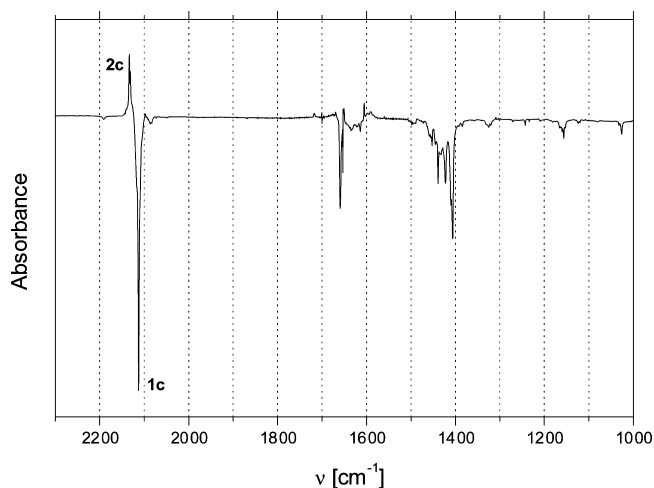
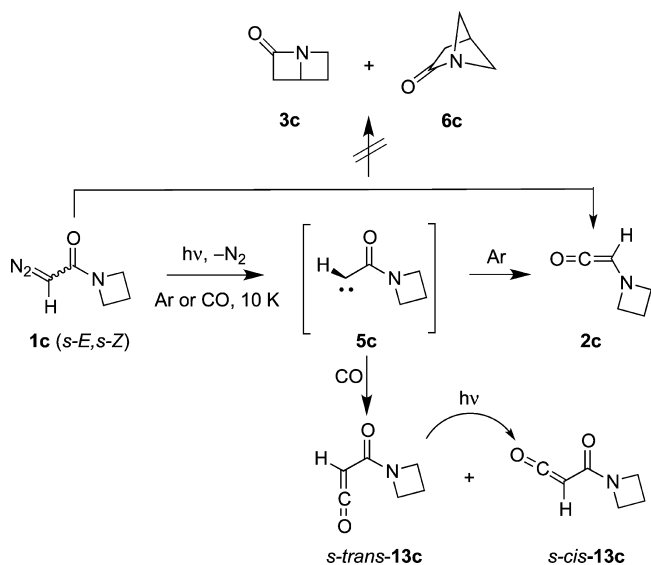


**Figure 5.** IR difference spectrum obtained after irradiation of *N*-diazoacetylazetidine (**1c**) (2113, 1658, 1407  $\text{cm}^{-1}$ ) at  $\lambda$  254 nm for 10 min in an Ar matrix at 10 K: (bottom) disappearing bands of **1c**; (top) appearing bands ascribed to azetidinyketene (**2c**) (2133  $\text{cm}^{-1}$ ; calculated value 2133  $\text{cm}^{-1}$  (Table 1)).

within 2  $\text{cm}^{-1}$  (see Table 1 and the Supporting Information). Therefore, it cannot be excluded that a trace of **6d** is hidden under the weak absorption due to **3d**, but if so, the amount would be very small. Since ketene **2d** with its most prominent band at 2134  $\text{cm}^{-1}$  is obviously the main product, the Wolff rearrangement route is clearly favored in this case as well (Scheme 9 and Figure 7).

In summary, the photochemical decomposition of diazoamides **1a–d** and matrix-IR spectroscopic investigation of the products reveal a crucial dependence of the rearrangement path on the molecular structure. Thus, open-chain *N,N*-dialkyldiazoacetamides **1a,b** unambiguously prefer intramolecular C–H insertion and show only little if any contribution of the Wolff rearrangement. In contrast, the incorporation of the amide nitrogen into a four- or five-membered ring in diazoamides **1c,d** effectively suppresses insertion reactions in favor of the Wolff rearrangement. The presence of free carbenes as intermediates

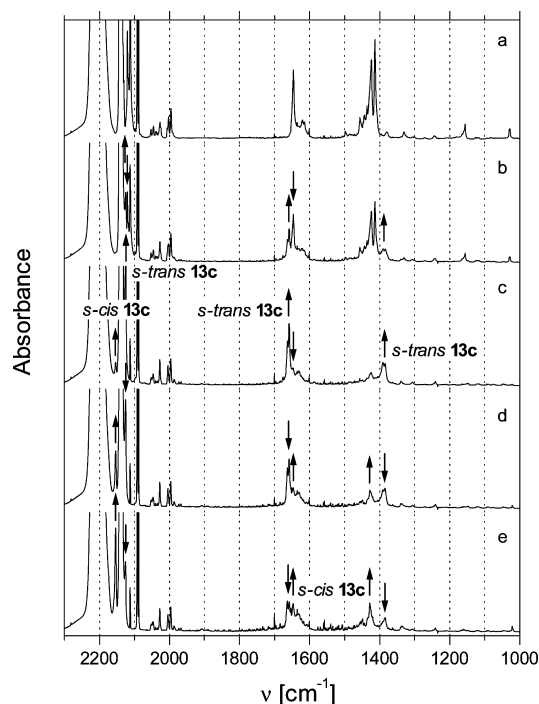
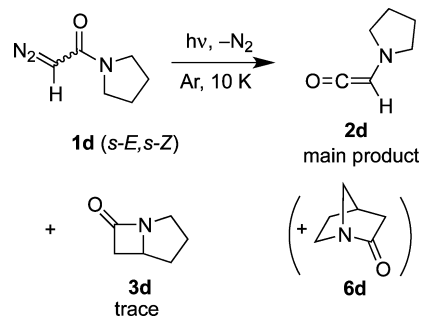


**Figure 6.** Course of the photochemical decomposition of *N*-diazoacetylazetidine (**1c**) (2120, 2112, 1646  $\text{cm}^{-1}$ ) in a CO matrix at 10 K: (a) deposition spectrum; (b–e) spectra after 5 min (b), 15 min (c), 45 min (d), and 135 min (e) irradiation at  $\lambda$  254 nm. Prolonged irradiation causes the complete conversion of the azetidinyketene *s-trans*-**13c** (2125, 1663  $\text{cm}^{-1}$ ) to *s-cis*-**13c** (2153, 1647  $\text{cm}^{-1}$ ). Decreasing absorptions of **1c** and increasing absorptions of *s-trans*-**13c** and *s-cis*-**13c** are indicated with arrows.

## Scheme 9. Matrix Photolysis of Diazoamide 1d



in these reactions was substantiated by trapping with carbon monoxide, although this does not exclude the possibility that some reactions may also occur by RIES.

**Thermal Decomposition of Diazoamides 1a–d.** FVT of *N,N*-dimethyldiazoacetamide **1a** at 330–630  $^{\circ}\text{C}$  with Ar matrix isolation of the products gave a mixture of carbon monoxide, ketene ( $\text{CH}_2\text{CO}$ ), *N*-methylmethanimine, methyl isocyanate, and ethylene (Scheme 10 and Figure 8). All compounds were identified by comparison with matrix spectra of reference samples or previously reported matrix spectra.<sup>14</sup> Similarly to the photodecomposition of **3a** outlined in Scheme 6, these products most likely stem from the corresponding thermal cleavage of *N*-methylazetidinone (**3a**). [2 + 2] Cycloreversion of **3a** can lead either to ketene and *N*-methylmethanimine or to methyl isocyanate and ethylene (Scheme 10). The relative ratios of the various decomposition products vary only slightly with increasing temperature. However, the formation of carbon

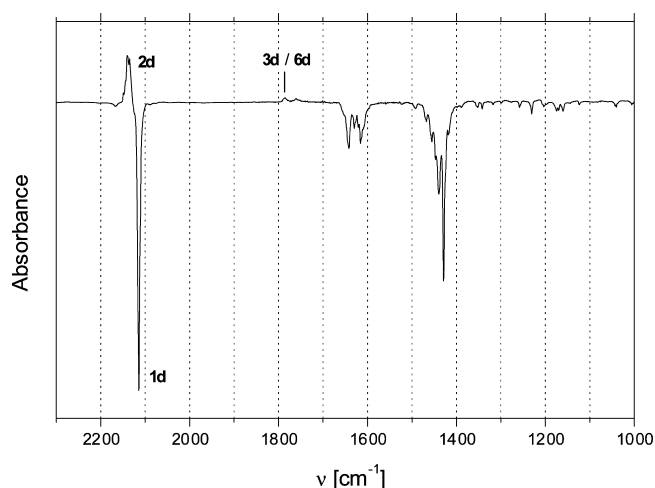
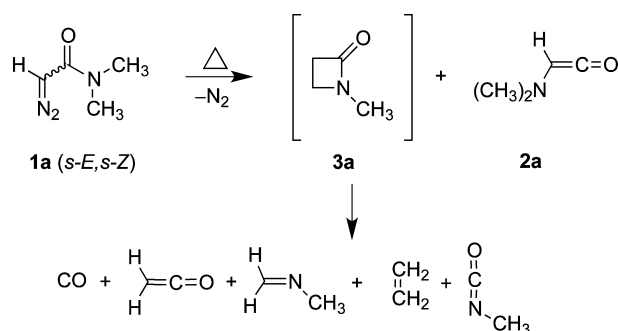


**Figure 7.** IR difference spectrum showing the photolysis of *N*-diazoacetylpyrrolidine **1d** matrix-isolated in argon at 10 K: (bottom) disappearing bands of **1d** (2112, 1430  $\text{cm}^{-1}$ ); (top) appearing bands of pyrrolidinyketene (**2d**) (2134  $\text{cm}^{-1}$ ; calculated value 2135  $\text{cm}^{-1}$  (Table 1)). Starting decomposition to CO gives rise to the peak at 2137  $\text{cm}^{-1}$  on the high-frequency side of **2d**. Weak bands at 1785–1761  $\text{cm}^{-1}$  are tentatively assigned to the C–H insertion product **3d** (cf. Figure 11). It is possible that a trace of **6d** is hidden under the weak signal due to **3d** (see text).

**Scheme 10. Thermal Formation of 3a and 2a and Decomposition of 3a by CO Elimination and [2 + 2] Cycloreversion**



monoxide and the [2 + 2] cycloreversion to methyl isocyanate and ethylene gain more importance at the expense of the alternative cleavage to ketene and *N*-methylmethanimine (in the photochemical reaction, formation of ketene and CO was preferred; vide supra). Formation of a small amount of aminoketene **2a** is indicated by a weak absorption at 2132  $\text{cm}^{-1}$ , which also gains intensity with increasing temperature (Figure 8).

As azetidinone **3a** cannot be isolated from the FVT reaction under these conditions, an alternative technique was sought. In pulsed pyrolysis experiments the sample is mixed with a carrier gas, e.g. argon, at a pressure of about 1 atm and then introduced through a pulsed valve into a short capillary pyrolysis tube at 1000–1200 °C. Just after the pyrolysis zone the resulting supersonic argon beam is allowed to expand into the high vacuum of the cryostat, thereby rapidly cooling the thermally excited primary pyrolysis products and allowing their observation in the deposited Ar matrix.<sup>15</sup> This technique is known to allow isolation of primary pyrolysis products which would not survive FVT conditions.<sup>16</sup> As the sample has to be mixed with the carrier gas, an essential prerequisite is a

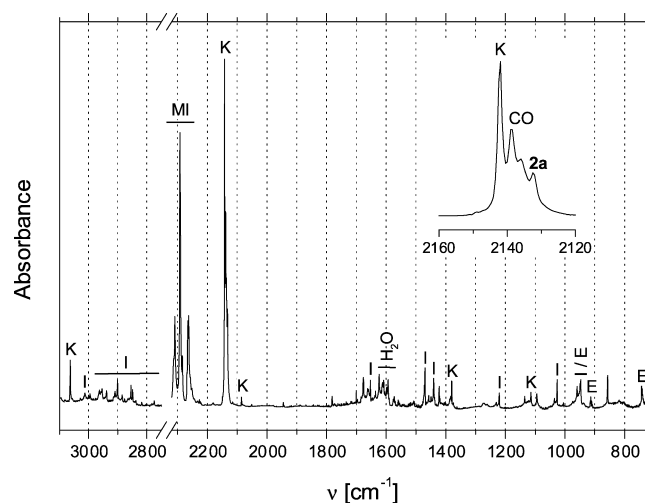


**Figure 8.** IR spectrum (argon, 14 K) of the products of FVT of *N,N*-dimethyldiazoacetamide (**1a**) at 500 °C. The inset shows an expansion of the 2160–2120  $\text{cm}^{-1}$  region. Legend: K, ketene ( $\text{CH}_2\text{CO}$ ); MI, methyl isocyanate; E, ethylene; I, *N*-methylmethanimine. **2a** appears at 2132  $\text{cm}^{-1}$ .<sup>14</sup>

sufficiently high vapor pressure of the sample. Since the diazoamide **1a** does not meet this requirement, a variation of the method was devised. When **1a** is heated in about 750 hPa of Ar, the yellow diazoamide starts to decompose at around 150 °C to form a more volatile compound, which enters the gas phase as a fine colorless mist and condenses on any cold surface. The thermolysis was performed in a glass tube attached to the pulsed valve, and the resulting gaseous product was deposited onto the 10 K KBr target (this is not a pulsed pyrolysis). The most prominent feature in the resulting IR spectrum is a characteristic set of carbonyl absorptions at 1781, 1775, and 1761  $\text{cm}^{-1}$ , belonging to *N*-methylazetidinone (**3a**) (Figure 9a). (This is in accord with the photolysis experiment depicted in Figure 1.) The correct assignment of these bands was proved by deposition of an authentic sample of **3a** (Figure

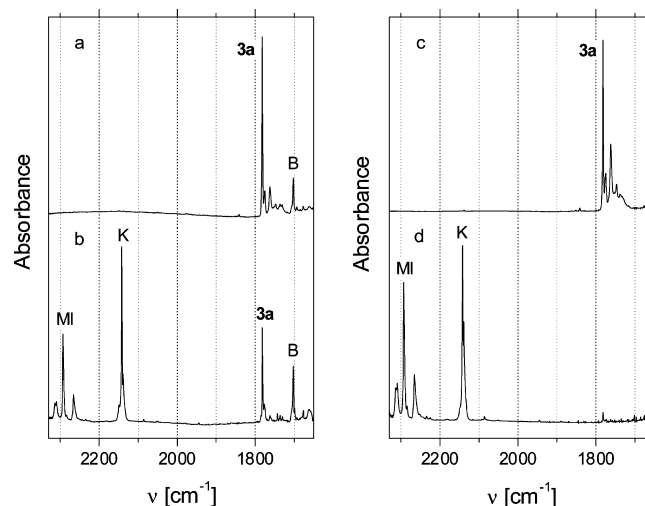


**Figure 9.** Matrix IR spectra (argon, 10 K): (a) *N*-methylazetidinone (**3a**) after thermolysis of *N,N*-dimethyldiazoacetamide (**1a**) at 150 °C in Ar with pulsed deposition; (b) same as (a) but with pulsed FVT prior to deposition; (c) authentic sample of **3a**; (d) pulsed FVT of authentic **3a**. Legend: K, ketene ( $\text{CH}_2\text{CO}$ ); MI, methyl isocyanate; B, unidentified carbonyl compound (1702  $\text{cm}^{-1}$ ).<sup>14</sup>

9c). Both the standard FVT of **1a** and pulsed pyrolysis of the gaseous product of the 150–170 °C thermolysis yield only decomposition products, largely methyl isocyanate and ketene (Figure 9b). *N*-Methylazetidione (**3a**) is volatile enough for pulsed pyrolysis, and the same bands due to decomposition products are again obtained (Figure 9d).

In contrast to **1a**, FVT of *N,N*-diethyldiazoacetamide (**1b**) at 400–500 °C with matrix isolation of the pyrolyzates gives detectable amounts of  $\beta$ - and  $\gamma$ -lactams. Thus, a mixture of the C–H insertion products **3b** and **6b**, carbon monoxide, and the products of thermal decomposition is obtained (Scheme 11 and

**Scheme 11. Formation and Thermal Decomposition of Lactams 3b and 6b**

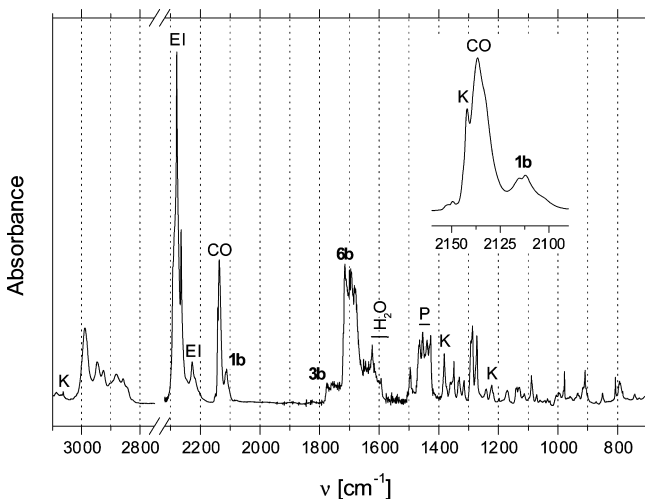
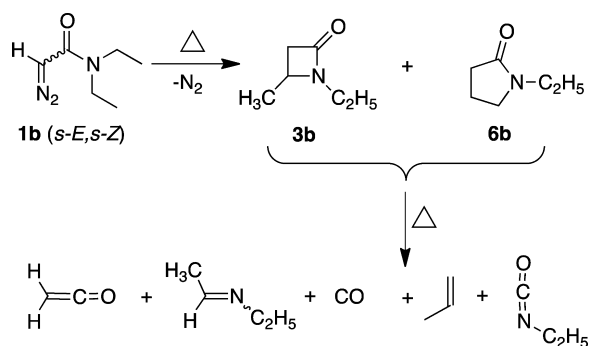


**Figure 10.** IR spectrum (argon, 7 K) of the products of FVT of *N,N*-diethyldiazoacetamide (**1b**) at 500 °C: residual **1b**, 2112  $\text{cm}^{-1}$ ; **3b**, 1775  $\text{cm}^{-1}$ ; **6b**, 1715  $\text{cm}^{-1}$ . The inset shows an expansion of the 2160–2090  $\text{cm}^{-1}$  region. Legend: K, ketene (2142  $\text{cm}^{-1}$ ); EI, ethyl isocyanate (2280, 2265  $\text{cm}^{-1}$ ); P, propene (1464, 1453, 1441  $\text{cm}^{-1}$ ); CO, 2137  $\text{cm}^{-1}$ .<sup>14</sup>

Figure 10; see also Figure S4 in the Supporting Information). The ability to detect **3b** under conditions where **3a** decomposes completely may be ascribed to the greater number of degrees of freedom in **3b** (and likewise in **6b**); i.e., these molecules are better able to dissipate the excess vibrational energy.

Very little if any diethylaminoketene (**2b**) is formed. At best, a shoulder at ca. 2132  $\text{cm}^{-1}$  on the stronger CO peak (2137  $\text{cm}^{-1}$ ) may be due to **2b** (Figure 10). The ratios of all observed compounds depend strongly on the temperature. The

decomposition of **1b** starts at approximately 350 °C under FVT conditions. The amounts of both lactams **3b** and **6b** decrease with increasing temperature, and their cleavage was complete on FVT at 600 °C. Interestingly, also the proportion of the [2 + 2] cycloreversion reaction to ketene and *N*-ethylethylideneamine decreases and vanishes at 600 °C. The [2 + 2] cycloreversion to ethyl isocyanate and propene dominates at all investigated temperatures (400–610 °C). The intensity of the CO signal increases with increasing temperature and thereby masks any possible formation of **2b**.

While *photolysis* of the matrix-isolated *N*-diazoacetylazetidine **1c** yielded aminoketene **2c** as a result of Wolff rearrangement, this ketene was not identifiable under thermal conditions. Unfortunately, FVT of **1c** above 300 °C leads to complete decomposition, with carbon monoxide as the only identified product.

Thermolysis of diazoacetylpyrrolidine (**1d**) at 150–170 °C in about 1 atm of Ar with pulsed deposition of the resulting gaseous product as described for **1a** above leads to complete decomposition and development of a new band at 1785  $\text{cm}^{-1}$  with shoulders at 1779 and 1761  $\text{cm}^{-1}$ , which all belong to the  $\beta$ -lactam **3d** (Scheme 12 and Figure 11). Because of the very

**Scheme 12. Thermal Formation and Decomposition of  $\beta$ -Lactam 3d and Possibly 6d**

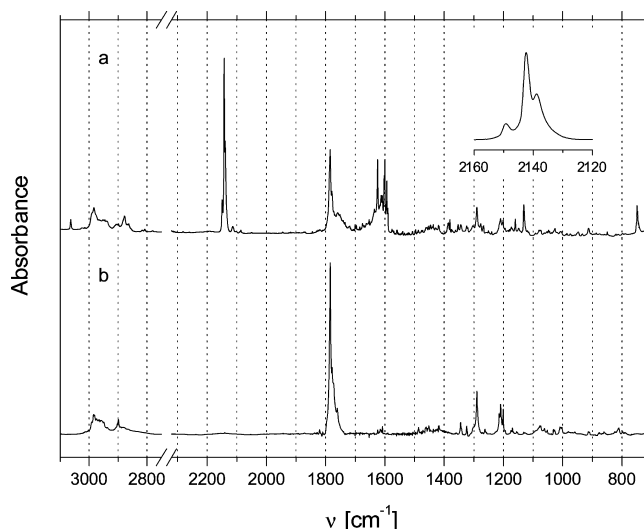
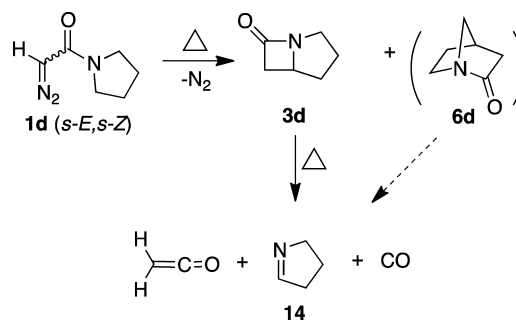


**Figure 11.** IR spectra (Ar, 10 K): (a) the product of thermolysis of *N*-diazoacetylpyrrolidine **1d** in Ar with pulsed deposition, largely **3d** (inset: bands due to ketene ( $\text{CH}_2\text{CO}$ ) and CO at 2142 and 2139/2149  $\text{cm}^{-1}$ );<sup>14</sup> (b) synthesized  $\beta$ -lactam **3d** (1785, 1779, 1761  $\text{cm}^{-1}$ ).

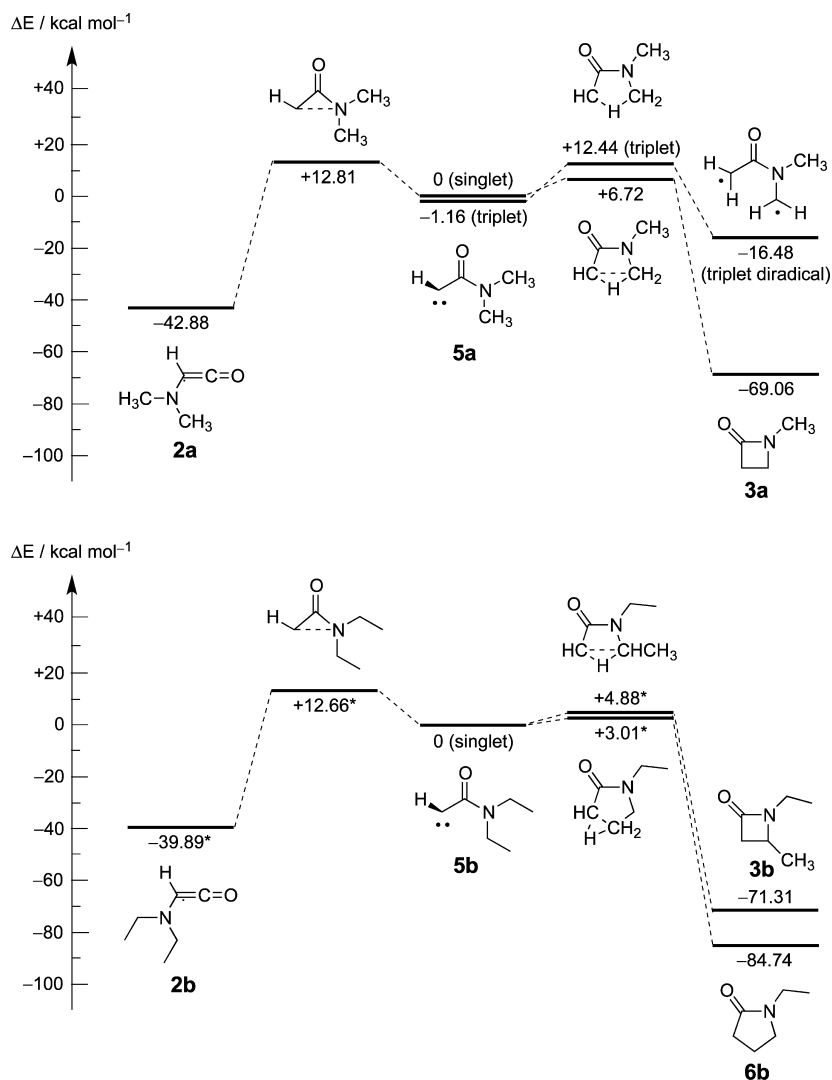


**Figure 12.** Relative calculated energies (kcal mol<sup>-1</sup>, B3LYP/6-31G(d)) of products and transition states arising from *N,N*-dimethyl- and *N,N*-diethyldiazoacetamides **1a,b**. In each series the respective singlet carbene **5** is set to 0 kcal mol<sup>-1</sup>; the value given for **2b** corresponds to its most stable conformer. Note: the carbene C–H bond is perpendicular to the planar amide moiety (see the Supporting Information for computational details).

similar calculated carbonyl absorption frequencies of **3d** and **6d** (Table 1), it cannot be excluded that the  $\gamma$ -lactam **6d** is present as well, but if so, it would only be a minor amount. Further strong bands at 2139/2149, 2142, and 1629 cm<sup>-1</sup> reveal the presence of CO, ketene (CH<sub>2</sub>CO), and 1-pyrroline (**14**), respectively. These compounds are formed by thermal fragmentation of **3d**, as demonstrated in separate experiments by FVT of a synthesized sample of **3d** at 500–700 °C. The decomposition of **3d** was complete only at 700 °C. The identity of 1-pyrroline (**14**) was confirmed by comparison with the matrix IR spectrum of an authentic sample. Ketene (CH<sub>2</sub>CO) and CO absorbed as usual at 2142 and 2137 cm<sup>-1</sup>, respectively. Again, in sharp contrast to the matrix photolysis, there is no clear evidence for the participation of a thermally induced Wolff rearrangement in the FVT of **1d**, although it is possible that a weak absorption due to aminoketene **2d** at 2134 cm<sup>-1</sup> could be hidden under the massif between 2130 and 2150 cm<sup>-1</sup> (Figure 11). Characteristic experimental and calculated wavenumbers of compounds **2**, **3**, and **6** are compared in Table 1.

## DISCUSSION

The interpretation of the experimental results is complicated by two factors: the possible occurrence of reactions in excited states (RIES) in the photochemical reactions (but not in the thermal ones) and the possibility of concerted Wolff rearrangements (WR) from diazoamide conformers with an *s-Z* relationship between the diazo and carbonyl groups.<sup>17</sup> Unlike the diazo esters,<sup>1,10</sup> the lowest energy conformer of the diazoamides **1** is the *s-Z* conformation (Scheme 1), which could favor concerted WR in the matrix photolysis experiments, but the barrier between *s-E* and *s-Z* conformers may easily be overcome in FVT experiments. In the following discussion we will primarily consider the reactions of the singlet carbenes.

*N,N*-Dimethyldiazoacetamide (**1a**) decomposes both photochemically and thermally to give predominantly *N*-methylazetidinone (**3a**) and only a small amount of *N,N*-dimethylaminoketene (**2a**). This suggests that C–H insertion is energetically favored with respect to the Wolff rearrangement, and at least in the FVT reactions it is a carbene process. Trapping of carbene **5a** with CO indicates that at least some carbenes are formed in the photolysis reactions, and the



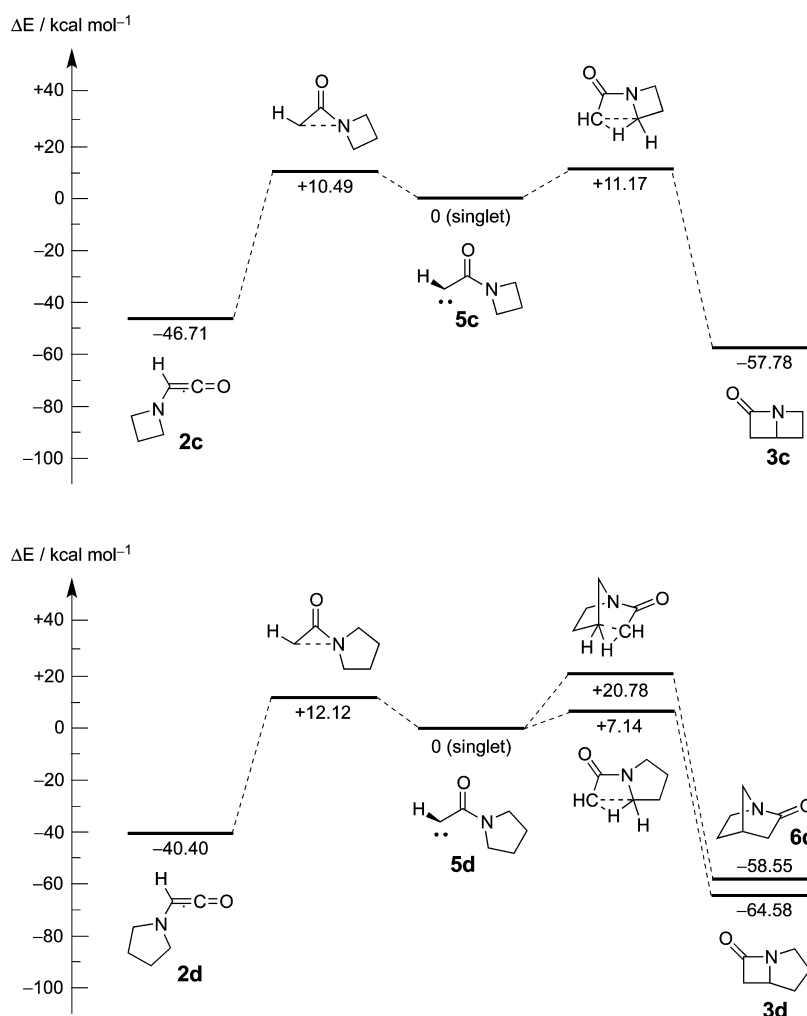
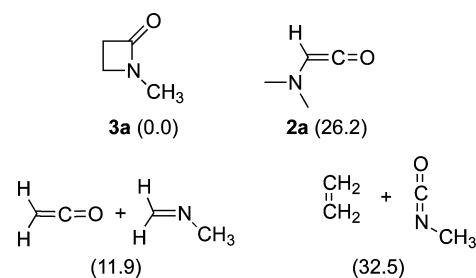


**Figure 13.** Relative calculated energies ( $\text{kcal mol}^{-1}$ , B3LYP/6-31G(d)) of products and transition states arising from diazoamides **1c,d**. For each series the respective singlet carbene **5** is set to 0  $\text{kcal mol}^{-1}$ . Note: the carbene C–H bond is perpendicular to the planar amide moiety (see the Supporting Information for computational details).

absence of aminoketene **2c** in the analogous trapping of **5c** with CO suggests that WR may in fact be a carbene process. DFT calculations for the potential carbene reactions show that the azetidinone **3a** is some  $26 \text{ kcal mol}^{-1}$  lower in energy than aminoketene **2a** (Figure 12). Nevertheless, formation of the ketene is possible, since the difference in activation barriers is only ca.  $6 \text{ kcal/mol}$  for the singlet and zero for the triplet carbene rearrangements (Figure 12). The calculated structures of carbene **5a** (in both its singlet and triplet states) are in favor of the insertion reactions: one hydrogen atom of the planar amide group comes close to a p orbital at the carbene center, in which the carbenic hydrogen atom is out of plane. Such nonplanar carbene structures have also been calculated for carbenic esters, e.g.  $^1\text{10}'$  (Scheme 3).<sup>10</sup> No minimum was found for a geometry with the amide methyl groups out of plane for either the singlet or the triplet state (B3LYP/6-31G(d) and UB3LYP/6-31G(d), calculations, respectively).

The fact that azetidinone **3a** could not be isolated in standard FVT experiments suggests that it is generated in a vibrationally excited state: i.e., chemically activated. This excess energy is sufficient for the fragmentation to the observed cycloreversion products, which lie ca. 12 and 33  $\text{kcal/mol}$  above **3a**, respectively (Chart 1). In the presence of 1 atm of argon the excess vibrational energy can be removed collisionally, and thus

**Chart 1.** Relative energies of  $\beta$ -lactam **3a** and its fragmentation products in  $\text{kcal/mol}$  (numbers in parentheses)



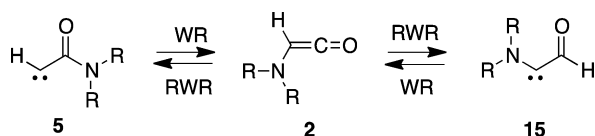
the primary thermolysis product **3a** can be observed. Since RIES is excluded, **3** must be formed in a C–H insertion reaction of the carbene in this case. Both singlet and triplet insertions are possible (Figure 12). The carbene has a calculated triplet ground state, but the singlet–triplet splitting is very small (Figure 12).

The results for *N,N*-diethyldiazoacetamide **1b** are analogous to those for the *N,N*-dimethyl case with C–H insertion to  $\beta$ - and  $\gamma$ -lactams **3b** and **6b** prevailing and the WR to aminoketene **2b** occurring only to a minor extent on photolysis. Although

the less strained five-membered-ring compound **6b** is thermodynamically favored by a calculated energy difference of 13 kcal mol<sup>-1</sup> (Figure 12), the four-membered-ring  $\beta$ -lactam **3b** predominates in the photolysis, but **6b** dominates in the thermolysis in accord with the thermochemistry (Figure 10 and Figure S4 (Supporting Information)).

In sharp contrast to the diazoacetamides **1a,b**, the incorporation of the amide nitrogen into a four- or five-membered ring in diazoamides **1c,d** effectively suppresses the C–H insertion reactions, thus leading to the formation of ketenes by WR on matrix photolysis. Since the intermediacy of carbenes in these reactions was confirmed by carbon monoxide trapping of **5a,c**, the WR is assumed to be at least in part a carbene reaction under these conditions. In contrast to the open chain alkyl-substituted carbenes, the approach of a C–H bond to the carbenic carbon is disfavored by the tied-back conformations of the methylene groups. Moreover, smaller ring C–H bonds have a higher degree of *s* character and are therefore stronger. The outcome is higher activation barriers for C–H insertion in **5c** (Figure 13). For the five-membered-ring system **5d** these effects are smaller, and the activation energies of WR and C–H insertion approach each other (Figure 13). The experimental results are in accord with this, since at least a trace of the C–H insertion products **3d** can be detected, whereas no C–H insertion is observed for **5c**.

**Scheme 13. Wolff (WR) and Potential Retro-Wolff (RWR) Rearrangements**



The near-exclusive formation of C–H insertion products in the *pyrolyses* of diazoacetamides **1a,b,d** demonstrates that purely thermal C–H insertion is perfectly feasible under conditions where RIES is excluded. The invariable formation of C–H insertion products in preference to ketenes is in agreement with the activation barriers for the carbene reactions, which are 5–7 kcal/mol higher for formation of ketenes **2a,b,d** than for the corresponding lactams (Figures 12 and 13). Unfortunately, compound **1c** decomposed on thermolysis, so that neither ketene nor lactam was observable. Only in the case of lactam **6d** is the activation barrier for its formation higher than that for the WR to aminoketene **2d**, and there was in fact no clear evidence for the formation of **6d**; instead, the energetically more favorable formation of lactam **3d** dominates (Figure 13). In addition to the lower activation barriers, the lactams also have significantly lower energies than the ketenes. Therefore, thermodynamic control of the reactions would be another reason for the low yields of thermal ketene formation. However, thermodynamic control would require that ketene formation be thermally reversible. This would correspond to a retro-Wolff rearrangement (Scheme 13). Retro-Wolff rearrangements (RWR) are known in cyclic iminoketenes, which under FVT conditions rearrange to cyclic iminocarbenes with calculated activation barriers of 37–44 kcal/mol.<sup>15,18</sup> It was shown recently that diaminoketenes can undergo RWR at room temperature.<sup>19</sup> However, in the present case, the calculations indicate activation barriers of the order of 50 kcal/mol for RWR (Figures 12 and 13). Although high, such barriers may be

overcome under the FVT conditions employed here, but the reaction would not be expected to occur under the static thermolysis conditions in Ar at 150 °C. A third possibility is that the ketenes disappear due to elimination of CO. Such processes are known as well, but they normally require temperatures above 500–600 °C in our apparatus,<sup>9,20</sup> and again they would not be expected under the static thermolysis conditions in Ar at 150 °C. It is noted that the putative RWR of ketenes **5** can proceed in two directions, to the original carbenes **5** and to the aminocarbenes **15** (Scheme 13). Furthermore, **5** and **15** can in principle interconvert via an oxirene. Nothing is known about FVT reactions of either aminoketenes or aminocarbenes, which are desirable topics for further investigation.

## CONCLUSION AND OUTLOOK

The photolyses of matrix-isolated diazoamides **1a–d** reveal a crucial dependence of the rearrangement path on the underlying molecular structure. Open-chain *N,N*-dialkyldiazoamides **1a,b** clearly prefer intramolecular C–H insertion and show only little formation of Wolff rearrangement (WR) products. In contrast, the incorporation of the amide nitrogen into a four- or five-membered ring in diazoamides **1c,d** effectively suppresses the insertion reactions in favor of the Wolff rearrangement to ketenes **2**. Calculations at the B3LYP level support the idea that the “tying-back” of the methylene groups, especially in the carbene **5c**, impedes C–H insertion, thereby favoring the WR energetically.

The presence of free carbenes in the photochemical reactions was substantiated by trapping with carbon monoxide.

Under FVT conditions the near-exclusive formation of C–H insertion products (lactams **3** and **6**) and/or their decomposition products arising from [2 + 2] cycloreversions is observed for diazoamides **1a,b,d**, and only **1a** affords a small amount of the aminoketene **2a**. This is in accord with the higher calculated activation barriers for WR relative to C–H insertion. Thus, the reactions reported here can be understood in terms of carbene reactivities, although it is emphasized that these experiments do not provide any information on the potential occurrence of reactions in the excited state (RIES) in the photochemical reactions or the concertedness of WR. We will show in forthcoming publications that suitably substituted diazoamides can in fact undergo substantial WR to aminoketenes under both photochemical and thermal conditions.

## EXPERIMENTAL SECTION

**General Methods.** Argon matrices were prepared by vacuum deposition of samples with argon (99.999%) onto a spectroscopic KBr target at about 30 K. Closed-cycle helium cryostats were used for matrix experiments. In FVT experiments, a mixture of argon and sample was led through a quartz tube (10 cm length, 0.8 cm inner diameter, equipped with heating wire and a thermocouple), and the products were subsequently isolated on the cold target at ca. 10 K. Procedures for pulsed pyrolysis have been described.<sup>15,16</sup> For thermolysis experiments under static argon pressure (750 hPa) the sample was placed in a glass tube. One end of the glass tube was connected to an electromagnetically operated pulsed valve, which was directly mounted on the head of the cryostat. The other end of the glass tube was connected to an argon reservoir. The sample was heated at the required temperature, and the resulting gaseous product was deposited onto the cold target by pulsing the electromagnetic valve. Photolyses were carried out using either a 1000 W Xe/Hg lamp in combination with cutoff filters or a low-pressure Hg arc lamp. Spectra were recorded at 7–10 K.

**Materials.** *N,N*-Dimethyldiazoacetamide (**1a**), *N,N*-diethyldiazoacetamide (**1b**), *N*-(diazooacetyl)azetidione (**1c**), and *N*-(diazooacetyl)pyrrolidine (**1d**) were prepared according to literature procedures.<sup>2,3,21,22</sup> *N*-Methylazetidione (**3a**),<sup>23</sup> 1-azabicyclo[3.2.0]heptan-7-one (**6b**),<sup>24</sup> and 1-pyrroline (**14**)<sup>25</sup> were prepared as reported.

**Matrix Experiments.** *N,N*-Dimethyldiazoacetamide (**1a**). IR (Ar, 7 K): 2963 (vw), 2949 (vw), 2938 (vw), 2919 (vw), 2898 (vw), 2880 (vw), 2860 (vw), 2115 (vs), 1677 (w), 1649 (m), 1638 (w), 1614 (w), 1496 (m), 1460 (w), 1441 (w), 1409 (m), 1397 (m), 1338 (vw), 1271 (vw), 1171 (w), 1127 (w), 1095 (vw), 1066 (vw), 1064 (vw), 915 (w), 913 (w), 910 (w), 908 (vw), 743 (m), 741 (w), 723 (w) cm<sup>-1</sup>.

**Photolysis of *N,N*-Dimethyldiazoacetamide (**1a**) in an Argon Matrix.** A sample of **1a** was codeposited with Ar at 25 K. Broadband photolysis at  $\lambda \geq 305$ –310 nm and 7 K yielded predominantly *N*-methylazetidione (**3a**) accompanied by minor amounts of *N,N*-dimethylaminoketene (**2a**), carbon monoxide, ketene, and possibly further decomposition products. IR (argon, 7 K): 2960 (w), 2948 (w), 2919 (vw), 2892 (vw), 2142 (ketene, vw), 2138 (CO, w), 2132 (**2a**, vw), 1780 (**3a**, s), 1776 (**3a**, w), 1774 (**3a**, w), 1761 (**3a**, w), 1683 (w), 1677 (w), 1388 (w), 1273 (vw), 1234 (vw), 1156 (vw), 1095 (vw), 1072 (w), 969 (vw), 915 (w), 913 (w), 910 (w), 908 (vw), 744 (m), 741 (w) cm<sup>-1</sup>. Prolonged irradiation or, more rapidly, reduction of the excitation wavelength to  $\lambda$  254 nm intensified the absorbances at 2142 (ketene), 2138 (CO), and 2132 cm<sup>-1</sup> (**2a**) with respect to the still dominant band of **3a** at 1780 cm<sup>-1</sup>.

**Photolysis of *N,N*-Dimethyldiazoacetamide (**1a**) in a Carbon Monoxide Matrix.** A sample of **1a** was codeposited with carbon monoxide at 30 K. Photolysis at 8 K and  $\lambda \geq 305$ –310 nm or, more rapidly, at 254 nm yielded a mixture of *N*-methylazetidione (**3a**) and both the *s*-cis and the *s*-trans conformers of *N,N*-dimethylaminocarbonylketene (**13a**). IR (CO, 8 K): **3a**, 1770 (s), 1392 (s), 1081 (vw) cm<sup>-1</sup>; *s*-cis-**13a**, 2155 (s), 1636 (m) cm<sup>-1</sup>; *s*-trans-**13a**, 1654 (m) cm<sup>-1</sup>. The absorption of the ketene function in *s*-trans-**13a** is covered by the CO bands. Irradiation also brings about a conformational change in favor of *s*-cis-**13a**.

**FVT of *N,N*-Dimethyldiazoacetamide (**1a**).** FVT of **1a** at various temperatures (330–630 °C) followed by Ar matrix isolation of the pyrolyzates gave mixtures of carbon monoxide, ketene, *N*-methylmethanimine, methyl isocyanate, and ethylene. IR (Ar, 14 K): carbon monoxide, 2138 (s) cm<sup>-1</sup>; ketene, 3063 (m), 2142 (vs), 2086 (w), 1380 (m), 1114 (w), 973 (vw) cm<sup>-1</sup>; *N*-methylmethanimine, 3014 (vw), 2964 (vw), 2955 (vw), 2940 (vw), 2902 (vw), 2886 (w), 2878 (vw), 2856 (vw), 2850 (w), 2839 (w), 2818 (vw), 2776 (vw), 1470 (m), 1441 (m), 1222 (w), 1027 (m), 950 (w) cm<sup>-1</sup>; methyl isocyanate, 2309 (m), 2292 (vs), 2284 (w), 2265 (m), 2263 (m) cm<sup>-1</sup>; ethylene, 1441 (m), 948 (m), 915 (w), 913 (m), 910 (w), 743 (m), 741 (m) cm<sup>-1</sup>; starting from ~450 °C, *N,N*-dimethylaminoketene (**2a**), 2132 (w) cm<sup>-1</sup>.

**Thermolysis of *N,N*-Dimethyldiazoacetamide (**1a**) in Argon with Pulsed Deposition.** A sample of **1a** was placed in a glass tube, which was attached to the cold head of a cryostat via an electromagnetic valve. After an atmosphere of about 750 hPa of Ar was applied to the system, the sample was heated to 150–170 °C, and the resulting gaseous product was deposited onto the cold window to yield *N*-methylazetidione (**3a**). IR (argon, 10 K): **3a**, 1841 (vw), 1782 (vs), 1775 (m), 1762 (m), 1573 (vw), 1557 (vw), 1496 (vw), 1474 (vw), 1417 (vw), 1388 (m), 1273 (w), 1236 (vw), 1072 (m), 968 (w), 811 (vw), 743 cm<sup>-1</sup>; unknown carbonyl compound, 1702 (m), 913 (w) cm<sup>-1</sup>.

**FVT of *N*-Methylazetidione (**3a**) produced by Thermolysis of **1a** in Argon.** The gaseous product from the aforementioned experiment containing **3a** was pulse-pyrolyzed, and the products were condensed on the cold window to yield ketene, *N*-methylmethanimine, methyl isocyanate and ethylene. IR data: see the data under FVT of **1a**.

***N*-Methylazetidione (**3a**).** An authentic sample of **3a** was codeposited with Ar at 10 K. IR (Ar, 10 K): 2959 (vw), 2911 (vw), 2892 (vw), 1841 (vw), 1782 (vs), 1775 (m), 1762 (s), 1747 (w), 1739 (w), 1572 (vw), 1557 (vw), 1492 (vw), 1474 (vw), 1416 (vw), 1388 (m), 1273 (w), 1236 (vw), 1086 (vw), 1071 (m), 968 (w), 811 (vw), 743 (vw), 547 (vw) cm<sup>-1</sup>.

**FVT of *N*-Methylazetidione (**3a**).** Pyrolysis of an authentic sample of **3a** followed by Ar matrix isolation of the products gave ketene, *N*-methylmethanimine, methyl isocyanate, and ethylene. IR (Ar, 10 K): ketene, 3064 (m), 2142 (vs), 1381 (m), 1115 (w), 525 (m); *N*-methylmethanimine, 1470 (m), 1441 (m), 1221 (w), 1027 (m); methyl isocyanate, 2309 (m), 2293 (s), 2266 (m); ethylene, 1441 (m), 948 (m) cm<sup>-1</sup>.

***N,N*-Diethyldiazoacetamide (**1b**).** IR (Ar, 8 K): 2986 (w), 2939 (w), 2112 (vs), 1639 (s), 1625 (sh), 1616 (sh), 1483 (m), 1461 (m), 1450 (m), 1442 (s), 1432 (s), 1382 (w), 1351 (m), 1311 (vw), 1257 (m), 1230 (w), 1167 (m), 1134 (m), 1098 (w), 1089 (w), 1077 (w), 952 (vw), 813 (vw), 779 (vw), 725 (w), 621 (vw), 417 (w) cm<sup>-1</sup>.

**Photolysis of *N,N*-Diethyldiazoacetamide (**1b**).** A sample of **1b** was codeposited with Ar at 25 K. Broad-band photolysis (Xe/Hg lamp) at 8 K yielded a mixture of 1-ethyl-4-methyl-2-azetidione (**3b**), 1-ethyl-2-pyrrolidinone (**6b**), and *N,N*-diethylaminoketene (**2b**). IR (argon, 8 K): 2985 (w), 2940 (w), 2903 (vw), 2880 (vw), 2132 (**2b**, w), 1775 (**3b**, vs), 1755 (**3b**, sh), 1716 (**6b**, m), 1593 (w), 1495 (vw), 1463 (w), 1446 (w), 1427 (w), 1411 (w), 1406 (w), 1396 (w), 1381 (w), 1355 (w), 1348 (w), 1332 (vw), 1315 (w), 1286 (w), 1271 (w), 1263 (w), 1241 (vw), 1214 (w), 1170 (vw), 1129 (vw), 1100 (vw), 1085 (w), 1070 (w), 1060 (w), 965 (vw), 942 (vw), 898 (vw), 850 (vw), 830 (vw), 812 (w), 788 (vw), 770 (vw), 654 (vw) cm<sup>-1</sup>. Prolonged irradiation or, more rapidly, reduction of the wavelength to  $\lambda \geq 190$  nm gave rise to new bands at 2289 (w), 2279 (w), 2266 (all due to ethyl isocyanate, w), 2142 (ketene, sh), 2138 (CO, s), 1680 (vw), 1658 (possibly ethylethylideneamine, vw), 1602 (m), 1593 (s), 1591 (s), 1453 (propylene, vw), and 1438 (propylene, vw) cm<sup>-1</sup>.

**FVT of *N,N*-Diethyldiazoacetamide (**1b**).** FVT of a sample of **1b** at 400–600 °C with Ar matrix isolation of the pyrolyzates gave a complex, temperature-dependent mixture of 1-ethyl-4-methyl-2-azetidione (**3b**), 1-ethyl-2-pyrrolidinone (**6b**), carbon monoxide, ketene, *N*-ethylethylideneamine, ethyl isocyanate, and propene. IR (argon, 7 K; intensity decreasing (↓) or increasing (↑) with increasing temperature): 2988 (m), 2947 (w), 2925 (w), 2881 (w), 2858 (vw), 2292 (ethyl isocyanate, sh), 2280 (ethyl isocyanate, vs), 2265 (ethyl isocyanate, s), 2228 (ethyl isocyanate, w), 2142 (ketene, ↓), 2138 (CO, ↑), 1775 (**3b**, ↓), 1715 (**6b**, ↓), 1693 (br, ↑), 1683 (br, ↑), 1496 (w), 1464 (m), 1453 (propene, m), 1441 (propene, m), 1427 (m), 1382 (w), 1350 (w), 1332 (vw), 1315 (vw), 1287 (m), 1272 (m), 1243 (vw), 1222 (vw), 1168 (vw), 1134 (vw), 1089 (vw), 978 (vw), 909 (vw), 850 (vw), 808 (vw), 793 (vw), 742 (vw), 650 (vw), 578 (vw), 524 (vw) cm<sup>-1</sup>.

**1-Azabicyclo[3.2.0]heptan-7-one (**6b**).** IR (Ar, 6 K): 2994 (w), 2982 (w), 2899 (w), 1784 (vs), 1778 (m/sh), 1761 (w/sh), 1487 (vw), 1461 (vw), 1452 (vw), 1417 (vw), 1345 (w), 1324 (w), 1290 (w), 1262 (vw), 1214 (w), 1209 (w), 1201 (w), 1002 (w), 609 (w), 549 (vw), and 456 (vw) cm<sup>-1</sup>.

**1-Pyrroline (**14**).** IR (Ar, 8 K): 3022 (vw), 2979 (s), 2963 (s), 2937 (s), 2877 (m), 1629 (s), 1474 (m), 1435 (m), 1321 (m), 1305 (w), 1280 (w), 1214 (m), 1081 (m), 1021 (m), 947 (m), 915 (m), 862 (w), 813 (w), 789 (w), and 412 (w) cm<sup>-1</sup>.

**FVT of 1-Azabicyclo[3.2.0]heptan-7-one (**6b**).** FVT at 500–700 °C with deposition of the products in an Ar matrix gave mixtures of undecomposed **6b**, ketene (CH<sub>2</sub>CO), 1-pyrroline (**14**), and CO. The bands due to **6b** disappeared completely only on FVT at ca. 800 °C.

***N*-(Diazooacetyl)azetidione (**1c**).** IR (Ar, 10 K): 3017 (vw), 2991 (vw), 2970 (vw), 2949 (vw), 2908 (w), 2890 (w), 2885 (vw), 2113 (vs), 1658 (s), 1653 (m), 1636 (w), 1618 (w), 1600 (w), 1453 (w), 1439 (m), 1423 (m), 1407 (s), 1362 (vw), 1325 (vw), 1302 (vw), 1271 (vw), 1243 (vw), 1217 (vw), 1161 (w), 1157 (w), 1124 (vw), 1120 (vw), 1027 (w), 895 (vw), 815 (vw), 722 (w), 541 (vw) cm<sup>-1</sup>.

**Photolysis of *N*-(Diazooacetyl)azetidione (**1c**) in an Argon Matrix.** A sample of **1c** was codeposited with Ar at 25 K. Photolysis at  $\lambda \geq 305$ –310 nm and 10 K or, more rapidly, irradiation at 254 nm and 10 K yielded azetidinyketene (**2c**). IR (argon, 10 K): 2133 (vs), 2131 (s) cm<sup>-1</sup>. Photolysis of **1c** at 254 nm was partially accompanied by decomposition of **2c** and gave rise to new signals at 2138 (CO, m), 2102 (w), 2098 (w), and 1718 (m) cm<sup>-1</sup>.

**Photolysis of *N*-(Diazoacetyl)azetidine (1c) in a Carbon Monoxide Matrix.** A sample of 1c was codeposited with carbon monoxide at 25 K. Photolysis at 10 K and  $\lambda$  254 nm yielded a mixture of the *s*-cis and the *s*-trans conformers of azetidinyldicarbonylketene (13c). IR (CO, 10 K): *s*-trans-13c, 2125 (s), 1663 (m), 1658 (m), 1391 (w), 1384 (w)  $\text{cm}^{-1}$ ; *s*-cis-13c, 2153 (s), 1647 (m), 1428 (w)  $\text{cm}^{-1}$ . Prolonged irradiation caused the complete conversion of *s*-trans-13c to *s*-cis-13c.

**FVT of *N*-(Diazoacetyl)azetidine (1c).** FVT of 1c at various temperatures (300–600 °C) followed by argon matrix isolation of the pyrolyzates resulted in complete and unspecific decomposition, with carbon monoxide being the only identifiable product.

***N*-(Diazoacetyl)pyrrolidine (1d).** IR (Ar, 10 K): 2992 (w), 2880 (w), 2114 (vs), 1642 (m), 1630 (sh), 1616 (m), 1455 (sh), 1440 (m), 1429 (s), 1258 (vw), 1231 (vw), 1204 (vw), 1175 (vw), 1160 (vw), 1124 (vw), 1040 (vw), 1006 (vw), 966 (vw), 915 (vw), 881 (vw), 732 (w), 518 (vw)  $\text{cm}^{-1}$ .

**Photolysis of *N*-(Diazoacetyl)pyrrolidine (1d).** A sample of 1d was codeposited with argon at 10 K. After photolysis with  $\lambda$  254 nm ketene 2d was observed at 2134  $\text{cm}^{-1}$  (Ar, 10 K).

**FVT of *N*-(Diazoacetyl)pyrrolidine (1d).** The FVT was carried out under the same conditions as described for 1a above. IR (argon, 10 K): 3064 (ketene, w), 2984 (w), 2878 (w), 2149 (m), 2142 (ketene, vs), 2139 (CO, s), 1785 (s), 1779 (m), 1760 (sh), 1600 (w), 1380 (ketene, w), 1290 (m), 1160 (w), 913 (vw), 749 (m), 590 (vw), 525 (vw)  $\text{cm}^{-1}$ .

## ■ ASSOCIATED CONTENT

### ● Supporting Information

Figures S1–S4, showing additional IR spectra from the photolysis of 1b, and figures and tables giving standard orientations, dipole moments, thermochemical data, and IR spectra of optimized structures at the (U)B3LYP/6-31G(d) level (thermochemistry at the B3LYP/6-311+G(3df,2p) level). This material is available free of charge via the Internet at <http://pubs.acs.org>.

## ■ AUTHOR INFORMATION

### Corresponding Author

\*E-mail for C.W.: [wentrup@uq.edu.au](mailto:wentrup@uq.edu.au).

### Notes

The authors declare no competing financial interest.

## ■ ACKNOWLEDGMENTS

We are indebted to Professor M. S. Platz (Ohio State University), who was instrumental in creating the collaboration between our laboratories, for discussions, and for providing samples of 1c. U.M. was a Feodor Lynen postdoctoral fellow and thanks the Alexander von Humboldt-Stiftung (Germany) for financial support. This work was also supported by the Australian Research Council and the National Computing Infrastructure facility (NCMAS g01) supported by the Australian Government.

## ■ REFERENCES

- (1) For reviews of the Wolff rearrangement see (a) Maier, H.; Zeller, K. *Angew. Chem., Int. Ed. Engl.* **1975**, *14*, 32–43. (b) Kirmse, W. *Eur. J. Org. Chem.* **2002**, 2193–2256.
- (2) Chaimovich, H.; Vaughan, R. J.; Westheimer, F. H. *J. Am. Chem. Soc.* **1968**, *90*, 4088–4093.
- (3) (a) Rando, R. R. *J. Am. Chem. Soc.* **1970**, *92*, 6706–6707. (b) Rando, R. R. *J. Am. Chem. Soc.* **1972**, *94*, 1629–1631.
- (4) (a) Tomioka, H.; Kitagawa, H.; Izawa, Y. *J. Org. Chem.* **1979**, *44*, 3072–3075. (b) Tomioka, H.; Kondo, M.; Izawa, Y. *J. Org. Chem.* **1981**, *46*, 1090–1094.
- (5) Corey, E. J.; Felix, A. M. *J. Am. Chem. Soc.* **1965**, *87*, 2518–2519.

- (6) (a) Doyle, M. P.; Forbes, D. C. *Chem. Rev.* **1998**, *98*, 911–936. (b) Doyle, M. P.; McKervey, M. A.; Ye, T. In *Modern Catalytic Methods for Organic Synthesis with Diazo Compounds*; Wiley: New York, 1998. (c) Davies, H. M. L.; Beckwith, R. E. *J. Chem. Rev.* **2003**, *103*, 2861. (d) Padwa, A.; Krumpke, K. E. *Tetrahedron* **1992**, *48*, 5385–5453. (e) Wee, A. G. H.; Duncan, S. C. *J. Org. Chem.* **2005**, *70*, 8372–8380. (f) Choi, M. K.-W.; Yu, W.-Y.; Che, C.-M. *Org. Lett.* **2005**, *7*, 1081–1084. (g) Zhang, W.; Wee, G. H. *Org. Lett.* **2010**, *12*, 5386–5389. (h) Slattery, C. N.; Ford, A.; Maguire, A. R. *Tetrahedron* **2010**, *66*, 6681–6705. (i) Kaupang, A.; Bonge-Hansen, T. *Beilstein J. Org. Chem.* **2013**, *9*, 1407–1413.
- (7) Franich, R. A.; Lowe, G.; Parker, J. J. *Chem. Soc., Perkin Trans. 1* **1972**, 2034–2041.
- (8) Richardson, D. C.; Hendrick, M. E.; Jones, M., Jr. *J. Am. Chem. Soc.* **1971**, *93*, 3790–3791. Kammula, S. L.; Tracer, H. L.; Shevlin, P. B.; Jones, M., Jr. *J. Org. Chem.* **1977**, *42*, 2931–2932.
- (9) Visser, P.; Zuhse, R.; Wong, M. W.; Wentrup, C. *J. Am. Chem. Soc.* **1996**, *118*, 12598–12602.
- (10) Zhang, Y.; Burdzinski, G.; Kubicki, J.; Platz, M. S. *J. Am. Chem. Soc.* **2009**, *131*, 9646.
- (11) (a) Zhu, Z.; Bally, T.; Stracener, L. L.; McMahon, R. J. T. *J. Am. Chem. Soc.* **1999**, *121*, 2863–2874. (b) Wang, Y.; Yuzawa, T.; Hamaguchi, H.; Toscano, J. P. *J. Am. Chem. Soc.* **1999**, *121*, 2875–2882. (c) Wang, J.-L.; Likhovtorik, I.; Platz, M. S. *J. Am. Chem. Soc.* **1999**, *121*, 2883–2890. (d) Zhang, Y.; Kubicki, J.; Wang, J.; Platz, M. S. *J. Phys. Chem. A* **2008**, *112*, 11093–11098. (e) Burdzinski, G.; Platz, M. S. *J. Phys. Org. Chem.* **2010**, *23*, 308–314.
- (12) See e.g.: (a) Baird, M. S.; Dunkin, I. R.; Hacker, N.; Poliakov, M.; Turner, J. J. *J. Am. Chem. Soc.* **1981**, *103*, 5190–5195. (b) West, P. R.; Chapman, O. L.; LeRoux, J.-P. *J. Am. Chem. Soc.* **1982**, *104*, 1779–1782.
- (13) Siemeling, U.; Färber, C.; Bruhn, C.; Leibold, M.; Selent, D.; Baumann, W.; von Hopffgarten, M.; Goedecke, C.; Frenking, G. *Chem. Sci.* **2010**, *1*, 697–704. Siemeling, U. *Aust. J. Chem.* **2011**, *64*, 1108.
- (14) Assignments of IR spectra of decomposition products were verified by reported data. Ethyl isocyanate: (a) Paraskewas, S. M.; Danopoulos, A. A. *Synthesis* **1983**, 638–640. (b) Mironov, V. F.; Kozyukov, V. P.; Orlov, G. I. *J. Gen. Chem. USSR (Engl. Trans.)* **1982**, *52*, 1870–1874; *Zh. Obshch. Khim.* **1982**, *52*, 2102–2106. Propene: (c) Radziszewski, J. G.; Downing, J. W.; Gudipati, M. S.; Balaji, V.; Thulstrup, E. W.; Michl, J. *J. Am. Chem. Soc.* **1996**, *118*, 10275–10284. (d) Nefedov, O. M.; Maltsev, A. K.; Khabashesku, V. N.; Korolev, V. A. *J. Organomet. Chem.* **1980**, *201*, 123–136. Ketene (e) Moore, C. B.; Pimentel, G. C. *J. Chem. Phys.* **1963**, *38*, 2816–2829. *N*-Ethylethylideneamine (f) Turovskii, A. A.; Kucher, R. V.; Kushch, O. V.; Turovskii, N. A. *J. Org. Chem. USSR (Engl. Transl.)* **1986**, *22*, 654–657; *Zh. Org. Khim.* **1986**, *22*, 732–736. (g) Stevens, C.; de Kimppe, N. *J. Org. Chem.* **1993**, *58*, 132–134. *N*-Methylmethanimine: (h) Bibas, H.; Koch, R.; Wentrup, C. *J. Org. Chem.* **1998**, *63*, 2619–2626. Methyl isocyanate: (i) Dunkin, I. R.; Shields, C. J.; Quast, H. *Tetrahedron* **1989**, *45*, 259–268. Ethylene: (j) Cowieson, D. R.; Barnes, A. J.; Orville-Thomas, W. J. *J. Raman Spectrosc.* **1981**, *10*, 224–226. CO (free,  $2137 \pm 1 \text{ cm}^{-1}$ ; water complex,  $2148 \text{ cm}^{-1}$ ): (k) Dubost, H.; Abouaf-Marguin, L. *Chem. Phys. Lett.* **1972**, *73*, 269. (l) Johnstone, D. E.; Sodeau, J. R. *J. Chem. Soc., Faraday Trans.* **1992**, *88*, 409–415.
- (15) Kohn, D. W.; Clauberg, H.; Chen, P. *Rev. Sci. Instrum.* **1992**, *63*, 4003–4005.
- (16) Qiao, G. G.; Meutermans, W.; Wong, M. W.; Träubel, M.; Wentrup, C. *J. Am. Chem. Soc.* **1996**, *118*, 3852–3861.
- (17) Kaplan, F.; Meloy, G. K. *J. Am. Chem. Soc.* **1966**, *88*, 950–956.
- (18) Nguyen, M. T.; Hajnal, M. R.; Vanquickenborne, L. G. *J. Chem. Soc., Perkin Trans. 2* **1994**, 169–170.
- (19) Schulz, T.; Färber, C.; Leibold, M.; Bruhn, C.; Baumann, W.; Selent, D.; Porsch, T.; Holthausen, M. C.; Siemeling, U. *Chem. Commun.* **2013**, *49*, 6834–6836.
- (20) Leung-Toung, R.; Wentrup, C. *Tetrahedron* **1992**, *48*, 7641–7654.

(21) (a) Aggarwal, V. K.; Blackburn, P.; Fieldhouse, R.; Jones, R. V. H. *Tetrahedron Lett.* **1998**, *39*, 8517–8520. (b) Regitz, M.; Hocker, J.; Liedhegener, A. *Organic Syntheses*; Wiley: New York, 1973; Collect. Vol. V, pp 179–182. (c) Garcia, J.; Gonzalez, J.; Segura, R.; Vilarrasa, J. *Tetrahedron* **1984**, *40*, 3121–3127.

(22) Sturm, H.; Ongania, K. H.; Daly, J. J.; Klötzer, W. *Chem. Ber.* **1981**, *114*, 190–200.

(23) (a) Holley, R. W.; Holley, A. D. *J. Am. Chem. Soc.* **1949**, *71*, 2124–2129. (b) Abboud, J.-L. M.; Cañada, T.; Homan, H.; Notario, R.; Cativiela, C.; Diaz de Villegas, M. D.; Bordejé, M. C.; Mó, O.; Yáñez, M. *J. Am. Chem. Soc.* **1992**, *114*, 4728–4736.

(24) Moll, F.; Thoma, H. Z. *Naturforsch., B* **1969**, *24*, 942–943.

(25) Bock, H.; Dammel, R. *Chem. Ber.* **1987**, *120*, 1971–1985.